Ceramic Membranes

International Edition: DOI: 10.1002/anie.201604035
German Edition: DOI: 10.1002/ange.201604035

A Dual-Phase Ceramic Membrane with Extremely High H_2 Permeation Flux Prepared by Autoseparation of a Ceramic Precursor

Shunfan Cheng, Yanjie Wang, Libin Zhuang, Jian Xue, Yanying Wei, Armin Feldhoff, Jürgen Caro,* and Haihui Wang**

Abstract: *A novel concept for the preparation of multiphase composite ceramics based on demixing of a single ceramic precursor has been developed and used for the synthesis of a dual-phase H_2-permeable ceramic membrane. The precursor $BaCe_{0.5}Fe_{0.5}O_{3-\delta}$ decomposes on calcination at 1370 °C for 10 h into two thermodynamically stable oxides with perovskite structures: the cerium-rich oxide $BaCe_{0.85}Fe_{0.15}O_{3-\delta}$ (BCF8515) and the iron-rich oxide $BaCe_{0.15}Fe_{0.85}O_{3-\delta}$ (BCF1585), 50 mol% each. In the resulting dual-phase material, the orthorhombic perovskite BCF8515 acts as the main proton conductor and the cubic perovskite BCF1585 as the main electron conductor. The dual-phase membrane shows an extremely high H_2 permeation flux of 0.76 mL min^{-1} cm^{-2} at 950 °C with 1.0 mm thickness. This auto-demixing concept should be applicable to the synthesis of other ionic-electronic conducting ceramics.*

Mixed protonic-electronic conducting (MPEC) ceramic materials are currently attracting increasing attention for their potential applications in hydrogen[1a–c] and humidity sensors,[1d,e] as well as hydrogen pumps.[1f,g] They can also be used as membranes for H_2 separation[1h–k] and in catalytic membrane reactors.[1l] Additionally, these materials can be used as electrolytes in solid-oxide fuel cells (SOFCs),[1m–q] as solid electrolytes for ammonia synthesis,[1r,s] and as photocatalysts for the decomposition of water.[1t]

Most MPEC materials are based on perovskite oxides and have the general formula ABO_3, such as $SrCeO_3$, $BaCeO_3$, $SrZrO_3$, $CaZrO_3$, and $SrTiO_3$. However, hydrogen permeation fluxes through such ceramic membranes cannot meet the industrial requirements, mainly because of poor electronic conductivity, even at high temperatures (800–950 °C).[2–4] Therefore, to improve the hydrogen permeation flux, trivalent elements, such as rare-earth elements, are doped into the B-sites of these oxides to improve their electronic conductivities. For example, elements such as Eu, Sm, Mn, and Nd are used in doped oxide systems based on $SrCeO_3$ and $BaCeO_3$.[5–7] Unfortunately, the hydrogen permeation fluxes through these single-phase membranes are still lower than 0.03 mL min^{-1} cm^{-2} because the hydrogen permeation rate is still limited mainly by the electronic conduction, even after metal doping. Another approach for improving the hydrogen permeation flux is to use a dual-phase membrane containing a second phase material to conduct electrons. Thus, many ceramic–metal (cermet) dual-phase materials, such as Ni-$BaCe_{0.9}Y_{0.1}O_{3-\delta}$,[8] Ni-$BaCe_{0.95}Tb_{0.05}O_{3-\delta}$,[9] and Ni-$BaZr_{0.1}Ce_{0.7}Y_{0.1}Yb_{0.1}O_{3-\delta}$,[10] composed of a ceramic protonic conductor and a metallic electronic conductor have been developed for hydrogen separation. The hydrogen permeation fluxes through these cermet membranes are one order of magnitude higher than those of single-phase membranes. The thermochemical stability and compatibility of the metal and ceramic are, however, critical.

As alternative options, ceramic–ceramic dual-phase membranes, such as $La_{5.5}WO_{11.25-\delta}$-$La_{0.87}Sr_{0.13}CrO_{3-\delta}$[1h] and $BaCe_{0.2}Zr_{0.7}Y_{0.1}O_{3-\delta}$ (BCZY27)-$Sr_{0.95}Ti_{0.9}Nb_{0.1}O_{3-\delta}$ (STN95)[11] have been developed in recent years. Normally, each single-phase oxide is prepared separately, and the oxides are homogenized by ball milling to obtain the dual-phase materials.[1h,i,11,12] However, it is difficult to preserve the phase purity in these composites at temperatures of 800–950 °C for a long period of time since the two phases can easily react with each other and cation diffusion occurs. For example, secondary phases appeared in the dual-phase ceramic membranes when using BCZY27 as the protonic conducting phase and STN95 as the electronic conducting phase.[11] Insufficient phase stability is indeed an undesired phenomenon among MPEC and mixed ionic and electronic conductive (MIEC) dual-phase membrane materials. For example, an interdiffusion zone at the interfaces between the $Ce_{0.85}Gd_{0.1}Cu_{0.05}O_{2-\delta}$ (CGCO) and $La_{0.6}Ca_{0.4}FeO_{3-\delta}$ (LCF) grains can be observed in the CGCO-LCF dual-phase membrane.[13] To enhance the ionic conductivity of the grain boundary, Lin et al.[12] reported targeted phase formation between two different phases. Liu et al.[14] also introduced nanoparticles for stabilization. Clearly, avoiding the formation of new miscellaneous phases between the different ceramic phases at high temperatures because of cation diffusion between the two phases is an important challenge that must be overcome for dual-phase membranes.

[*] S. Cheng, Y. Wang, L. Zhuang, Dr. Y. Wei, Prof. H. Wang
School of Chemistry and Chemical Engineering
South China University of Technology
510640 Guangzhou (China)
E-mail: ceyywei@scut.edu.cn
hhwang@scut.edu.cn
Dr. J. Xue, Dr. Y. Wei, Prof. A. Feldhoff, Prof. J. Caro
Institute of Physical Chemistry and Electrochemistry
Leibniz University of Hannover
Callinstrasse 3A, 30167 Hannover (Germany)
E-mail: juergen.caro@pci.uni-hannover.de
Prof. H. Wang
School of Chemical Engineering
The University of Adelaide
Adelaide, SA 5005 (Australia)

Supporting information for this article can be found under: http://dx.doi.org/10.1002/anie.201604035.

Herein, we propose a novel concept for the design and preparation of dual-phase membranes. The two phases contain the same chemical elements but in different concentrations and with different crystallographic symmetries. The iron-doped $BaCeO_3$ system is selected to demonstrate this concept because of its good proton conductivity.[15] A ceramic precursor of the starting composition $BaCe_{0.5}Fe_{0.5}O_{3-\delta}$ automatically decomposes on calcination into two thermodynamically stable oxides, the cerium-rich oxide $BaCe_{0.85}Fe_{0.15}O_{3-\delta}$ (BCF8515) and the iron-rich oxide $BaCe_{0.15}Fe_{0.85}O_{3-\delta}$ (BCF1585). The resulting dual-phase membrane consists of the orthorhombic perovskite BCF8515 and the cubic perovskite BCF1585 (Figure 1). In this dual-phase mixture, the

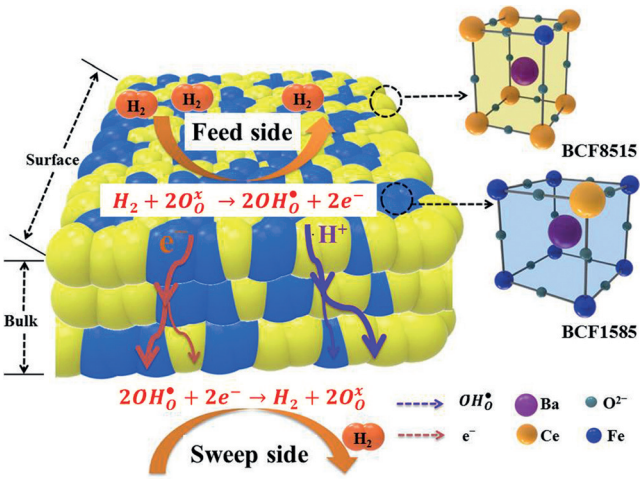

Figure 1. Concept of a dual-phase mixed protonic and electronic conducting membrane, which consists of two phases with the same elemental composition but in different concentration ratios that is prepared by the novel autoseparation method: The precursor $BaCe_{0.5}Fe_{0.5}O_{3-\delta}$ decomposes into the cerium-rich oxide $BaCe_{0.85}Fe_{0.15}O_{3-\delta}$ (BCF8515) as the proton conductor and the iron-rich oxide $BaCe_{0.15}Fe_{0.85}O_{3-\delta}$ (BCF1585) as the electron conductor. $OH_o^\bullet$ is the protonated lattice oxygen.

BCF8515 phase is the main protonic conductor, and the BCF1585 phase the main electronic conductor. This interplay of ambipolar conductivity results in a high hydrogen permeation flux. As illustrated in Figure 1, protons and electrons can be transported in both phases simultaneously, thus increasing the conductivity and also enlarging the triple phase boundary for the hydrogen surface exchange reaction [Eq. (1)]. Furthermore, secondary phase formation and cation diffusion between the two thermodynamically phases do not occur because of their limited solubility to ions.

$$H_2 + 2\,O_o^x \leftrightarrow 2\,OH_o^\bullet + 2\,e^- \qquad (1)$$

The ceramic precursor of the starting composition $BaCe_{0.5}Fe_{0.5}O_{3-\delta}$ was calcined at 1370 °C. Analysis of the XRD data (Figure 2) shows the as-synthesized dual-phase membrane decomposes into an equimolar mixture of the two phases BCF8515 and BCF1585. BCF8515 is an orthorhombic perovskite and BCF1585 a cubic perovskite.

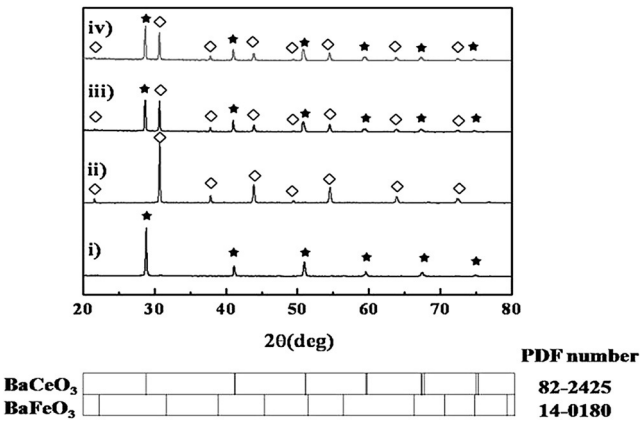

Figure 2. XRD patterns of different iron-containing barium cerate ceramics i) BCF8515 single-phase membrane; ii) BCF1585 single-phase membrane; iii) BCF8515-BCF1585 dual-phase membrane prepared by traditional ball-milling method; iv) BCF8515-BCF1585 dual-phase membrane prepared by the novel autoseparation method. All samples were calcined at 1370 °C for 10 h in air.

For comparison, we also prepared the composite ceramic BCF8515-BCF1585 by the traditional method. Thus, the two perovskites BCF8515 and BCF 1585 were synthesized separately, mixed in equimolar amounts as powders, homogenized by ball-milling, and calcined in air at 1370 °C. The novel autoseparation method gives the same phase structures (Figure 2) consisting of orthorhombic and cubic perovskite (sample iv) as the dual-phase membrane prepared by traditional ball-milling (sample iii).

To understand the reason underlying the interesting nature of the "coexisting-dual-phase", a series of $BaCe_{(1-x)}Fe_xO_{3-\delta}$ $(0.1 \le x \le 0.9)$ oxides was prepared, and the phase structures were investigated after calcination at 1370 °C. A pure perovskite structure could be obtained with Fe contents below 0.15 or above 0.8 (see Figure S1 in the Supporting Information). For Fe contents between 0.15 and 0.8, calcination resulted in the coexistence of the orthorhombic and cubic perovskite phases (see Figure S2). This difference is attributed to the large differences between the radii of Ce^{3+} and Ce^{4+} (1.15 and 1.01 Å) and Fe^{2+}, Fe^{3+}, and Fe^{4+} (0.92, 0.785, and 0.725 Å).[16,17] The differences in the radii are the reasons that the precursor $BaCe_{(1-x)}Fe_xO_{3-\delta}$ $(0.15 \le x \le 0.8)$ can autoseparate into the two phases of BCF1585 and BCF8515 and the dual-phase iron-doped $BaCeO_3$ oxides can be prepared by decomposition of the precursor. The secondary electron and backscattered electron micrographs (SEM and BSEM, respectively) of the BCF8515-BCF1585 dual-phase membrane exhibit distinct grain morphology and clear grain boundaries between the two phases (Figure 3).

The hydrogen permeation fluxes through the BCF8515-BCF1585 dual-phase membrane prepared by the autoseparation method are shown in Figure 4. A H_2 permeation flux of 0.76 mL min^{-1} cm^{-2} was obtained at 950 °C with a 1.0 mm thick dual-phase membrane. This effect arises from the good match between the protonic and electronic conductivities of each phase across the entire membrane, which leads to the BCF8515-BCF1585 dual-phase membrane exhibiting a high ambipolar conductivity. To clarify the contributions of the two

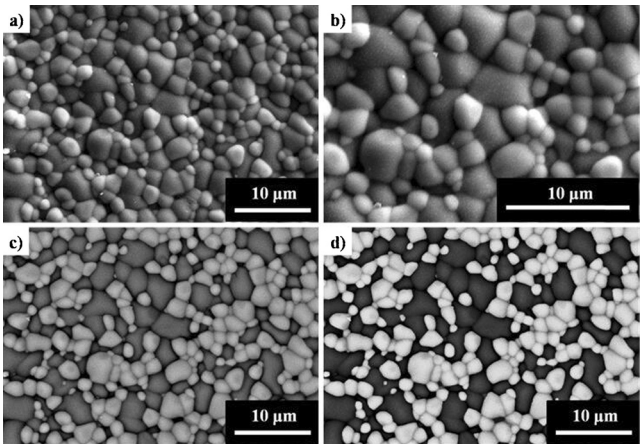

Figure 3. a) Secondary electron micrographs under a low-power lens. b) Secondary electron micrographs under a high-power lens. c) Backscattered electron micrographs (BSEMs) and d) the processed BSEM images of (c). The light particles are BCF8515 and the dark particles are BCF1585.

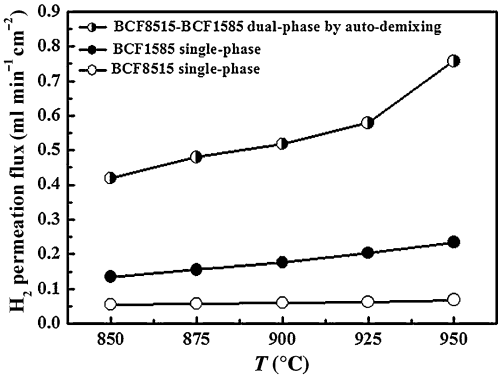

Figure 4. Comparison of hydrogen permeation flux through the dual-phase membrane and each single-phase membrane at different temperatures. Conditions: Total flow rate of 50% H_2 + 50% He on the feed side was 100 mL min^{-1}, and the Ar flow rate on the sweep side was 60 mL min^{-1}. Membrane thickness: 1.0 mm.

phases to the protonic and electronic conductivities, H_2 permeation fluxes through neat single-phase membranes of BCF8515 and BCF1585 were also studied (Figure 4). As expected, the dual-phase membrane exhibited a much higher H_2 permeation flux compared to either of the two single-phase membranes. This is because electronic conductivity is the limiting factor for the single-phase BCF8515 material, which is used as the main protonic conductor in the dual-phase membrane, while protonic conductivity is the limiting factor for single-phase BCF1585, which is used as the main electronic conductor in the dual-phase membrane. Therefore, the BCF8515-BCF1585 dual-phase membrane has a highly improved ambipolar conductivity and can achieve an extremely high H_2 permeation flux. The ambipolar conductivities of single-phase BCF8515 and BCF1585 as well as dual-phase BCF8515-BCF1585 membranes are shown in Figure S5 (see the Supporting Information).

The BCF8515-BCF1585 dual-phase membrane was also found to act as a dual ion conductor, exhibiting simultaneous proton and oxygen ion mobility (Figure S6). The oxygen permeation flux through the BCF8515-BCF1585 dual-phase membrane can reach 0.12 mL min^{-1} cm^{-2} at 950 °C. Similar to the $BaCe_{0.85}Tb_{0.05}Co_{0.1}O_{3-\delta}$ membrane,[18] the BCF8515-BCF1585 dual-phase membrane exhibits H_2 and O_2 permeability under different operating conditions. Although this MPEC material can transport both protons and oxygen ions, its H_2 selectivity does not decrease. By controlling the atmospheres on both sides of the membrane, H_2 permeation can be achieved exclusively (a more detail explanation can be found in Figure S7). This finding shows for the first time that that some oxygen-permeable materials could also be used for H_2 separation, if they are stable under reducing atmosphere.

Figure 5 and Table S1 summarize the H_2 permeation fluxes through the most relevant ceramic or cermet membranes. Although the measurement conditions used to study the various membranes differed, it is clear that the BCF8515-BCF1585 dual-phase membrane with a thickness of 1.0 mm exhibits extremely high hydrogen permeation flux compared with most other membranes under similar conditions. Higher hydrogen permeation flux through the dual-phase ceramic membrane can be obtained easily by decreasing the membrane thickness or enlarging the surface area by a coating.

In conclusion, we propose a novel preparation concept for dual-phase H_2-permeable membrane materials. A starting ceramic precursor with the composition $BaCe_{0.5}Fe_{0.5}O_{3-\delta}$ auto-decomposes upon heating at 1370 °C into a ceria-rich and an iron-rich phase. The two phases show different crystallographic structures and they co-exist for a long period of time. As a consequence of the composition of the

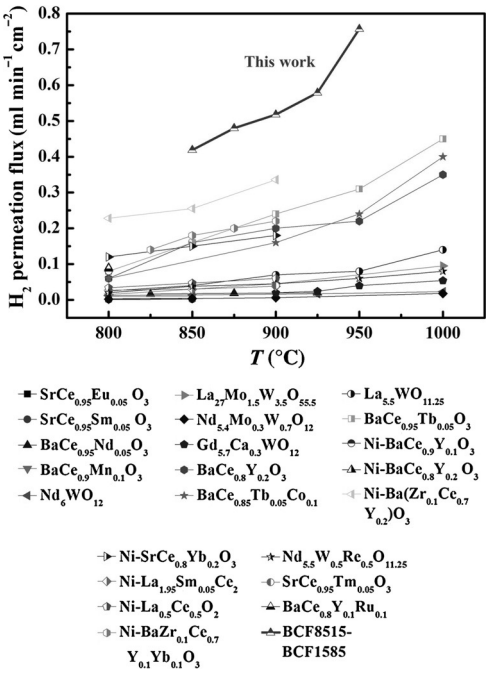

Figure 5. Comparison of hydrogen permeation properties of ceramic membranes: Single and dual-phase ceramics as well as cermet membranes.[5–7, 8, 10, 18, 19a–p] Conditions can be found in Table S1 in the Supporting Information. For our work: feed gas: 100 mL min^{-1} of (50% H_2 + 50% He), sweep gas: 60 mL min^{-1} of Ar, 1.0 mm thick disk membrane without surface coating, in a dry atmospheres.

starting ceramic, the resulting dual-phase ceramic consists of 50 mol% BCF8515 and 50 mol% BCF1585. The dual-phase membrane exhibits an extremely high hydrogen permeation flux of 0.76 mL min^{-1} cm^{-2} at 950 °C at a thickness of 1.0 mm. Thus, this material is a promising candidate for industrial high-temperature hydrogen separation or for catalytic membrane reactors. Our concept of using the autoseparation of precursors to obtain thermodynamically stable dual-phase ceramic materials is not only suitable for H_2-permeable membrane materials, but also for the preparation of O_2-permeable membrane materials. The auto-decomposition technique represents a new approach for the design and preparation of ceramic dual-phase mixed ionic and electronic conducting materials.

Acknowledgements

This study was supported by the Natural Science Foundation of China for Distinguished Young Scholars of China (no. 21225625), Natural Science Foundation of China (21536005), and the Natural Science Foundation of the Guangdong Province (2014A030312007). We thank the Sino-German Center for Science Promotion, Beijing, project GZ 911. Y.W. also greatly acknowledges the support by the Alexander von Humboldt Foundation. Support in TEM analysis by Frank Steinbach is acknowledged. We also thank Hongbin Chen for technical assistance.

Keywords: ceramic membranes · dual-phase composites · electron conductors · hydrogen permeation · proton conductors

How to cite: *Angew. Chem. Int. Ed.* **2016**, *55*, 10895–10898
Angew. Chem. **2016**, *128*, 11055–11058

[1] a) H. Iwahara, Y. Asakura, K. Katahira, M. Tanaka, *Solid State Ionics* **2004**, *168*, 299–310; b) N. Taniguchi, T. Kuroha, C. Nishimura, K. Lijima, *Solid State Ionics* **2005**, *176*, 2979–2983; c) Z. Y. Tang, X. G. Li, J. H. Yang, J. Yu, J. Wang, Z. N. Tang, *Sens. Actuators B* **2014**, *195*, 520–525; d) W. S. Wang, A. Vitae, A. V. Virkar, *Sens. Actuators B* **2004**, *98*, 282–290; e) J. Zhao, Y. P. Liu, X. W. Li, G. Y. Lu, L. You, X. S. Liang, F. M. Liu, T. Zhang, Y. Du, *Sens. Actuators B* **2013**, *181*, 802–809; f) H. Uchida, H. Kimura, H. Iwahara, *J. Appl. Electrochem.* **1990**, *20*, 390–394; g) Y. Kawamura, K. Isobe, T. Yamanishi, *Fusion Eng. Des.* **2007**, *82*, 113–121; h) S. Escolástico, C. Solís, C. Kjølseth, J. M. Serra, *Energy Environ. Sci.* **2014**, *7*, 3736–3746; i) E. Rebollo, C. Mortalo, S. Escolastico, S. Boldrini, S. Barison, J. M. Serra, M. Fabrizioa, *Energy Environ. Sci.* **2015**, *8*, 3675–3686; j) Y. Wei, J. Xue, H. Wang, J. Caro, *Chem. Commun.* **2015**, *51*, 11619–11621; k) Y. Wei, J. Xue, W. Fang, Y. Chen, H. Wang, J. Caro, *J. Membr. Sci.* **2015**, *488*, 173–181; l) Y. T. Liu, X. Y. Tan, K. Li, *Cat. Rev.* **2006**, *48*, 145–198; m) L. Yang, S. Wang, K. Blinn, M. Liu, Z. Liu, Z. Cheng, M. Liu, *Science* **2009**, *326*, 126–129; n) L. Bi, E. Fabbri, Z. Q. Sun, E. Traversa, *Energy Environ. Sci.* **2011**, *4*, 409–412; o) L. Bi, E. Fabbri, Z. Q. Sun, E. Traversa, *Solid State Ionics* **2011**, *196*, 59–64; p) E. Fabbri, B. Lei, D. Pergolesi, E. Traversa, *Adv. Mater.* **2012**, *24*, 195–208; q) T. Yajima, K. Koide, H. Takai, N. Fukatsu, H. Iwahara, *Solid State Ionics* **1995**, *79*, 333–337; r) Z. J. Li, R. Q. Liu, J. D. Wang, Y. H. Xie, F. Yue, *J. Solid State Electrochem.* **2005**, *9*, 201–204; s) J. L. Yin, X. W. Wang, J. H. Xu, H. T. Wang, F. Zhang, G. L. Ma, *Solid State Ionics* **2011**, *185*, 6–10; t) K. M. Parida, K. H. Reddy, S. Martha, D. P. Das, N. Biswal, *Int. J. Hydrogen Energy* **2010**, *35*, 12161–12168.
[2] R. C. T. Slade, N. Singh, *Solid State Ionics* **1993**, *61*, 111–114.
[3] H. Iwahara, T. Yajima, T. Hibino, K. Ozaki, H. Suzuki, *Solid State Ionics* **1993**, *61*, 65–69.
[4] N. Sata, K. Hiramoto, M. Ishigame, S. Hosoya, N. Niimura, S. Shin, *Phys. Rev. B* **1996**, *54*, 15795–15799.
[5] S. J. Song, E. D. Wachsman, J. Rhodes, S. E. Dorris, U. Balachandran, *Solid State Ionics* **2004**, *167*, 99–105.
[6] G. T. Li, G. X. Xiong, S. S. Sheng, W. S. Yang, *Chin. Chem. Lett.* **2001**, *12*, 937–940.
[7] M. Y. Cai, S. Liu, K. Efimov, J. Caro, A. Feldhoff, H. H. Wang, *J. Membr. Sci.* **2009**, *343*, 90–96.
[8] H. Kim, B. Kim, J. Lee, K. Ahn, H. R. Kim, K. J. Yoon, B. K. Kim, Y. W. Cho, H. W. Lee, J. H. Lee, *Ceram. Int.* **2014**, *40*, 4117–4126.
[9] X. X. Meng, J. Song, N. T. Yang, B. Meng, X. Y. Tan, Z. F. Ma, K. Li, *J. Membr. Sci.* **2012**, *401*, 300–305.
[10] S. M. Fang, K. Brinkman, F. L. Chen, *ACS Appl. Mater. Interfaces* **2014**, *6*, 725–730.
[11] J. S. Fish, S. Ricote, F. Lenrick, L. R. Wallenberg, T. C. Holgate, R. O'Hayre, N. Bonanos, *J. Mater. Sci.* **2013**, *48*, 6177–6185.
[12] Y. Lin, S. M. Fang, D. Su, K. S. Brinkman, F. L. Chen, *Nat. Commun.* **2015**, *6*, 6824.
[13] W. Fang, F. Y. Liang, Z. W. Cao, F. Steinbach, A. Feldhoff, *Angew. Chem. Int. Ed.* **2015**, *54*, 4847–4850; *Angew. Chem.* **2015**, *127*, 4929–4932.
[14] Y. Liu, X. F. Zhu, M. R. Li, R. P. O'Hayre, W. S. Yang, *Nano Lett.* **2015**, *15*, 7678–7683.
[15] H. Iwahara, Y. Asakura, K. Katahira, M. Tanaka, *Solid State Ionics* **2004**, *168*, 299–310.
[16] X. F. Zhu, H. H. Wang, W. S. Yang, *Chem. Commun.* **2004**, 1130–1131.
[17] X. F. Zhu, Y. Cong, W. S. Yang, *J. Membr. Sci.* **2006**, *283*, 158–163.
[18] J. Song, L. Li, X. Tan, K. Li, *Int. J. Hydrogen Energy* **2013**, *38*, 7904–7912.
[19] a) S. Escolástico, V. B. Vert, J. M. Serra, *Chem. Mater.* **2009**, *21*, 3079–3089; b) E. Vøllestad, C. K. Vigen, A. Magrasó, R. Haugsrud, *J. Membr. Sci.* **2014**, *461*, 81–88; c) Z. A. Li, C. Kjølseth, R. Haugsrud, *J. Membr. Sci.* **2015**, *476*, 105–111; d) W. Xing, P. Rauwel, C. H. Hervoches, Z. A. Li, R. Haugsrud, *Solid State Ionics* **2014**, *261*, 87–94; e) X. H. Tan, X. Y. Tan, N. T. Yang, B. Meng, K. Zhang, S. M. Liu, *Ceram. Int.* **2014**, *40*, 3131–3138; f) M. Marrony, *Proton Conducting Ceramics: From Fundamentals to Applied Research*, CRC Press, Taylor Francis Group, **2015**; g) S. Escolástico, C. Solís, T. Scherb, G. Schumacher, J. M. Serra, *J. Membr. Sci.* **2013**, *444*, 276–284; h) X. Y. Tan, J. Song, X. X. Meng, B. Meng, *J. Eur. Ceram. Soc.* **2012**, *32*, 2351–2357; i) C. D. Zuo, S. E. Dorris, U. Balachandran, M. L. Liu, *Chem. Mater.* **2006**, *18*, 4647–4650; j) Z. W. Zhu, W. P. Sun, L. T. Yan, W. F. Liu, W. Liu, *Int. J. Hydrogen Energy* **2011**, *36*, 6337–6342; k) S. J. Song, T. H. Lee, E. D. Wachsman, L. Chen, S. E. Dorris, U. Balachandrana, *J. Electrochem. Soc.* **2005**, *152*, J125–J129; l) L. T. Yan, W. P. Sun, L. Bi, S. M. Fang, Z. T. Tao, W. Liu, *Int. J. Hydrogen Energy* **2010**, *35*, 4508–4511; m) Z. W. Zhu, L. T. Yan, H. W. Liu, W. P. Sun, Q. P. Zhang, W. Liu, *Int. J. Hydrogen Energy* **2012**, *37*, 12708–12713; n) S. Escolástico, S. Somacescu, J. M. Serra, *Chem. Mater.* **2014**, *26*, 982–992; o) X. W. Qi, Y. S. Lin, *Solid State Ionics* **2000**, *130*, 149–156; p) H. Matsumoto, T. Shimura, T. Higuchi, *J. Electroanal. Chem.* **2005**, *152*, A488–A492.

Received: April 26, 2016
Published online: July 27, 2016

